Duke University
DURHAM
NORTH CAROLINA

Proposal 0136

DEPARTMENT OF PHYSICS

March 27, 1972

Mr. Donald R. Getz
Secretary
NAL Program Advisory Committee
National Accelerator Laboratory
P. O. Box 500
Batavia, Illinois 60510

Dear Don:

I would be happy to withdraw our proposal No. 136 if it is the one that I think it is, which was submitted last April for use of a hybrid system (30" bubble chamber plus spark chamber) with high energy π mesons. I do not want to withdraw my proposal No. 163, which is a proposal for the study of high energy π^1s with neon.

With best regards,

Yours sincerely,

Bill

W. D. Walker
Professor of Physics

WDW:jl

NAL PROPOSAL No. 0136

Scientific Spokesman:
W. D. Walker
Department of Physics
Duke University
Durham, North Carolina 27706

FTS/Off-net: 8 -919-286-0411
684-8111 ext. 8228

A STUDY OF HIGH ENERGY π - NUCLEON COLLISIONS

D. Carpenter, L. Fortney, C. Rose, W. D. Walker
Duke University

A. W. Key, J. D. Prentice, E. C. West, T. S. Yoon
University of Toronto

A. R. Erwin, M. A. Thompson
University of Wisconsin

April 28, 1971

PROPOSAL

A STUDY OF HIGH ENERGY π - NUCLEON COLLISIONS

Duke University

D. Carpenter, L. Fortney, C. Rose, W. D. Walker

University of Toronto

A. W. Key, J. D. Prentice, E. C. West, T. S. Yoon

University of Wisconsin

A. R. Erwin, M. A. Thompson

We propose to study π-nucleon collisions at 200 BeV using the 30" Hydrogen bubble chamber and wide gap spark chambers. We propose to take 600,000 pictures divided equally among π^+, π^- on p and π^+ on d. Up to 20 % of the pictures can be taken with very little peripheral equipment. An important feature of the proposal is in the detection of high energy γ-rays.

I. INTRODUCTION

We propose to use the 30" Bubble Chamber and associated upstream and downstream equipment to study general features of the reactions induced in π-nucleon interactions. We request a total of 600,000 pictures divided equally between $\pi^- - p$, $\pi^+ + p$, and $\pi^+ + D$ at 200 BeV with the equipment described below and at this intermediate energy we can measure many of the interesting dynamical variables sufficiently accurately to test several current theories of high energy reactions. Some of these answers can be obtained with the bubble chamber even if the downstream equipment and some of the upstream equipment is not available, but much more interesting physics will result if it is in operation. We are interested in obtaining up to 20 percent of our pictures with essentially no auxiliary downstream equipment.

Particularly, we shall measure the momentum distribution of produced pions formed in pion nucleon collisions. This information can only be obtained at NAL. This physics is discussed in Section 2.

We shall also be able to study diffraction dissociation of the nucleon and the diffraction dissociation of the π into various products as discussed in Section 3.

Our proposed system of gamma-ray detection from π^o will allow us to extend present knowledge of elastic and inelastic $\pi - \pi$ scattering by

identifying and studying some of the events $\pi + \pi \rightarrow$ even number of pions in the final state (Section 4).

We shall be able to search for quarks in three ways: 1) by identifying less than minimum ionizing track by charge of e/3 or 2e/3. 2) by detecting decay of quarks if their lifetime is in the range of 10^{-11} to 10^{-9} seconds, and 3) by observing traumatic changes in cross-sections as a function of mass. This is elaborated in Section 5.

In Section 6 we discuss the additional equipment that we propose to detect and measure the position of energetic gamma-rays and to improve the trigger system. We also discuss the importance of gamma-detection in event analysis. The bulk of the upstream and downstream equipment could be used by all experimental groups as discussed in the Appendix.

II. MULTIPION PRODUCTION

For strong interaction physics one of the principal advantages of the NAL accelerator over the ISR is its exclusive ability to study high energy meson-nucleon interactions. These interactions are perhaps more interesting than nucleon-nucleon interactions because they allow one to contrast features of hadron interactions which reflect the different structure of the nucleon and meson. For example, if the mesons have a 2-quark structure and the nucleons have a 3-quark structure, this quark-like structure would be most easily observed in meson-nucleon multiparticle production.*

The bare 30" ANL chamber is a very limited device, but several important questions in multiparticle physics can be answered using it without any additional downstream equipment. Part of our running time can be accumulated in this unadorned mode and still yield important results for multiparticle physics. In what follows we discuss the utility of the chamber without downstream equipment, however we intend to implement and use such equipment as much as possible to increase the accuracy of the data.

---

*Elbert et al., Phys. Rev., May D1 (1971).

Multiparticle Studies Without Downstream Equipment

By restricting the fiducial volume of the 30" chamber to the first 10 inches and using the full 30 KG field, it becomes possible to make many useful multiparticle studies without any auxiliary downstream equipment. We make the assumption that beam tracks are 200 GeV/c and that angular and position measurements are no better than obtained at ZGS energies.

A 200 GeV/c "leading" particle after the collision can have transverse momentum measured to 400 MeV/c which is right in the peak of the distribution of p_T. All slower particles will therefore have p_T determined well enough for many purposes. Longitudinal momentum will not be so well defined, but it does not have to be since the physically relevant variable seems to be $p_L/p_{max} = x$. Even a 20 percent measurement of this variable will answer a number of questions posed by lower energy data.

The value of the x variable runs from -1.0 to +1.0. Measurement errors for this variable are small for values of $x < +0.5$, becoming about 15 percent at $x = +0.5$. Above $x = +0.5$ the error soars to between 50 percent and 100 percent at $x = +1.0$. This is not serious for two reasons. 1) The large error occurs only at $x = +1.0$. Thus x cannot be greater than 1.0 nor as small as $x = +0.5$. 2) Only "leading" particles have this large

a value of x anyhow. Each event will have on the average approximately 1/2 a leading particle. The advantage of a positive primary beam is that negative secondary tracks are all produced pions and contain no fast (x = 1.0) "leading" pions.

Suppose the "ideal" spectrum for positive particles appears like this:

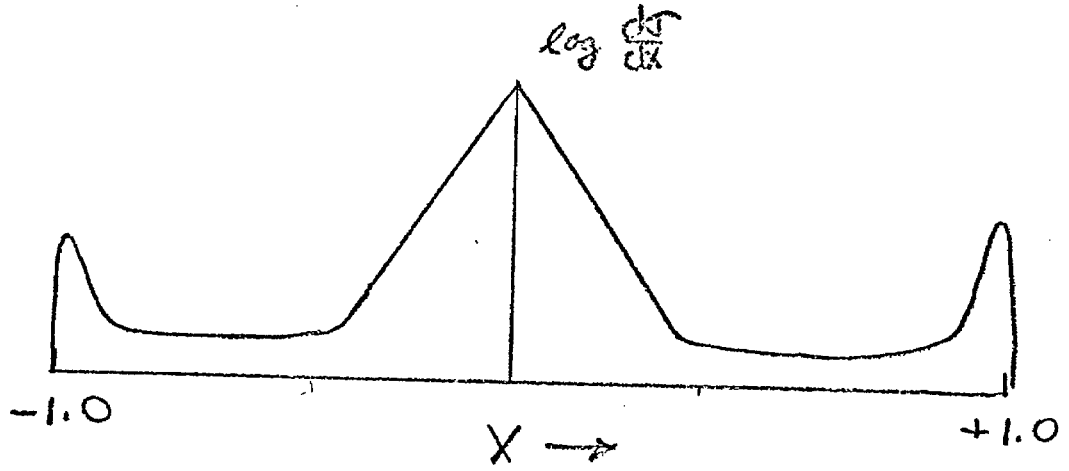

Our measured spectrum with a bare chamber would appear like this:

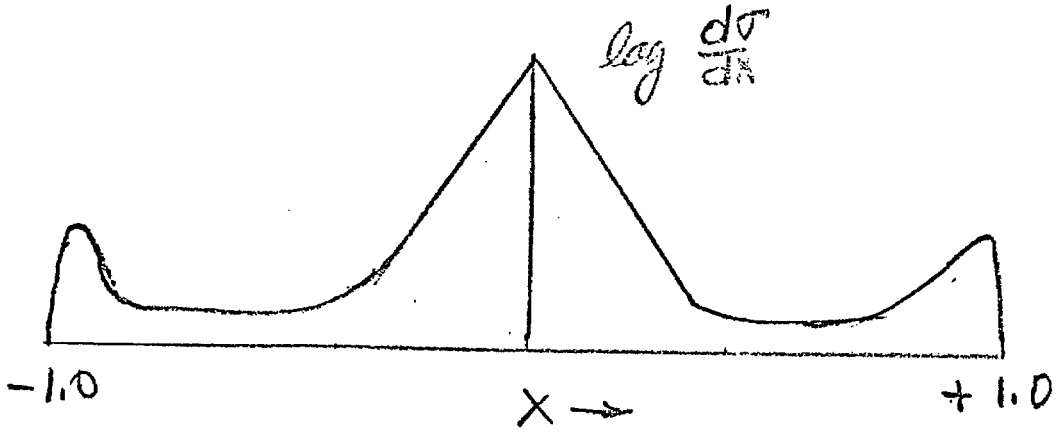

For "produced" negative pions we should be able to reproduce the "ideal" spectrum with no difficulty:

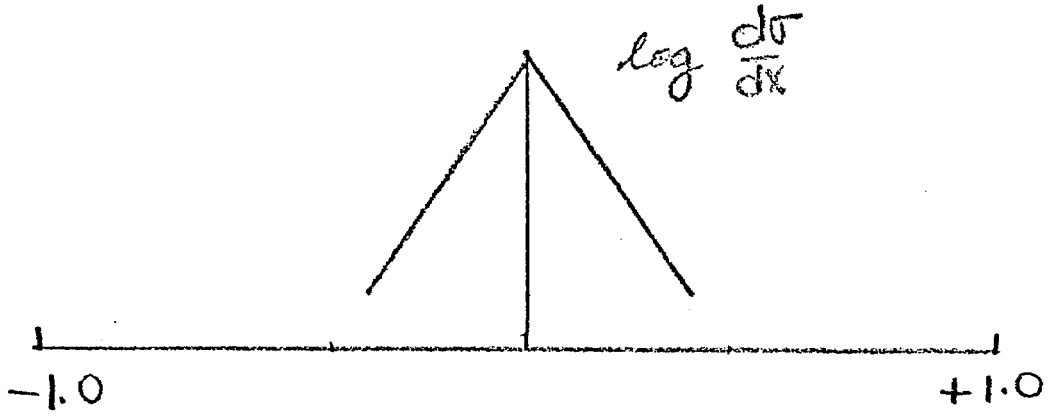

This faithful reproduction of the negative spectrum means we can detect the asymmetry in the produced pions which can be attributed to the difference in meson and nucleon quark structure.

Multiplicity distributions are particularly important for distinguishing some theories. The spatial resolution in the 30" chamber is still adequate for this at 200 GeV/c. A "worst-case" of two superimposed 100 GeV/c tracks of opposite sign would separate several bubble diameters in the 20" measuring region (assuming 20X demagnification and a 30 μ diffraction image on the film). We note that the optics in the 30" chamber are good enough to allow one to distinguish and measure by hand superimposed tracks separated by less than a bubble diameter.

In studying the possible high momentum track confusion we might encounter at 200 GeV/c, we have made a plot of the projected spatial

separation of the two closest tracks of each event as they leave the fiducial volume (Figure 1). This uses 25 GeV/c events scaled to 200 GeV/c. Only in less than 10 percent of the events do we find tracks closer than 4 track-widths. Scanning and measuring may be difficult in some cases but seldom impossible.

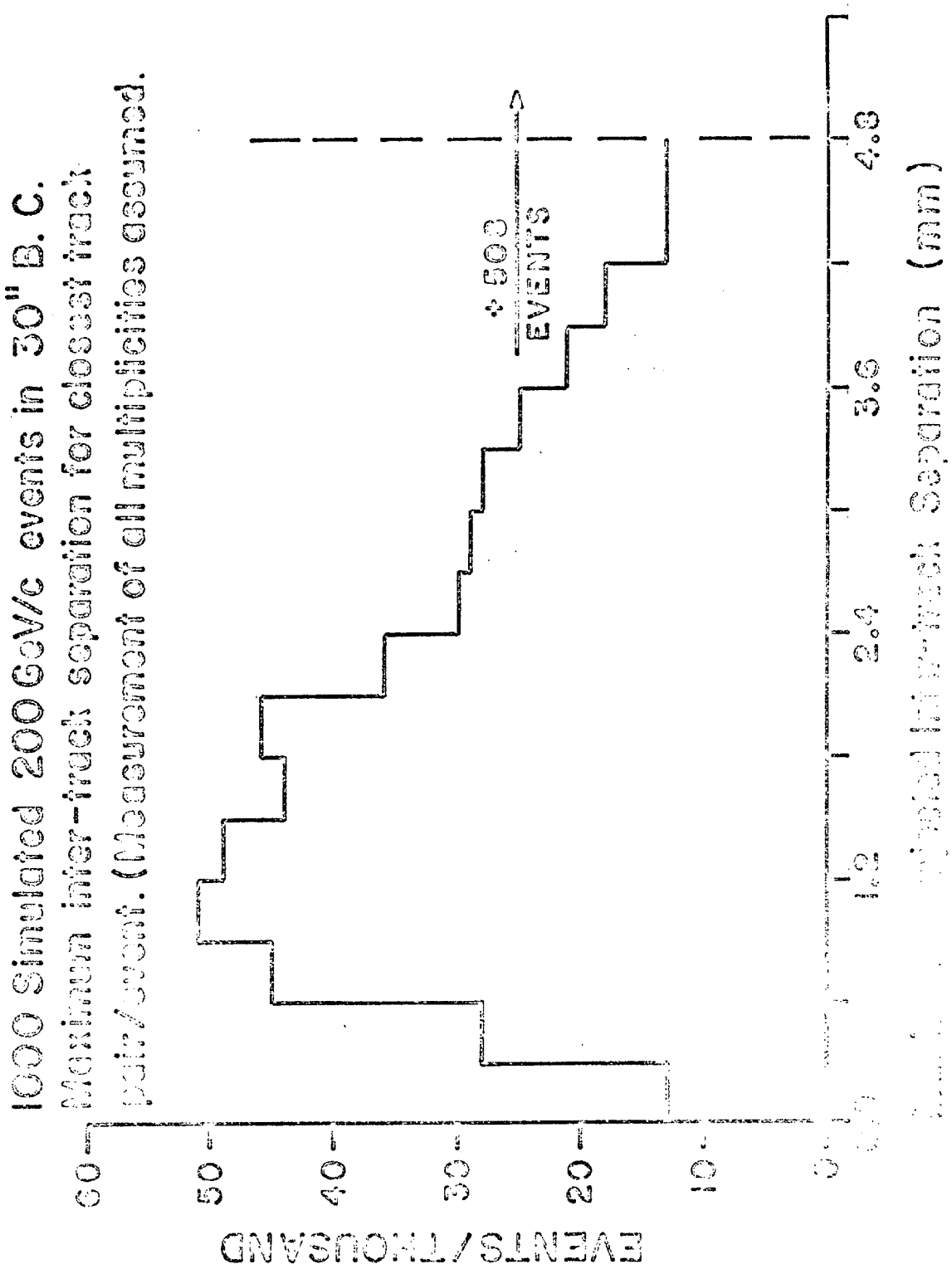
1000 Simulated 200 GeV/c events in 30" B. C.
Maximum inter-track separation for closest track pair/event. (Measurement of all multiplicities assumed.
+503
EVENTS
EVENTS/THOUSAND
60
50
40
30
20
10
1.2
2.4
3.6
4.8
Maximal Inter-track Separation (mm)

figure 1

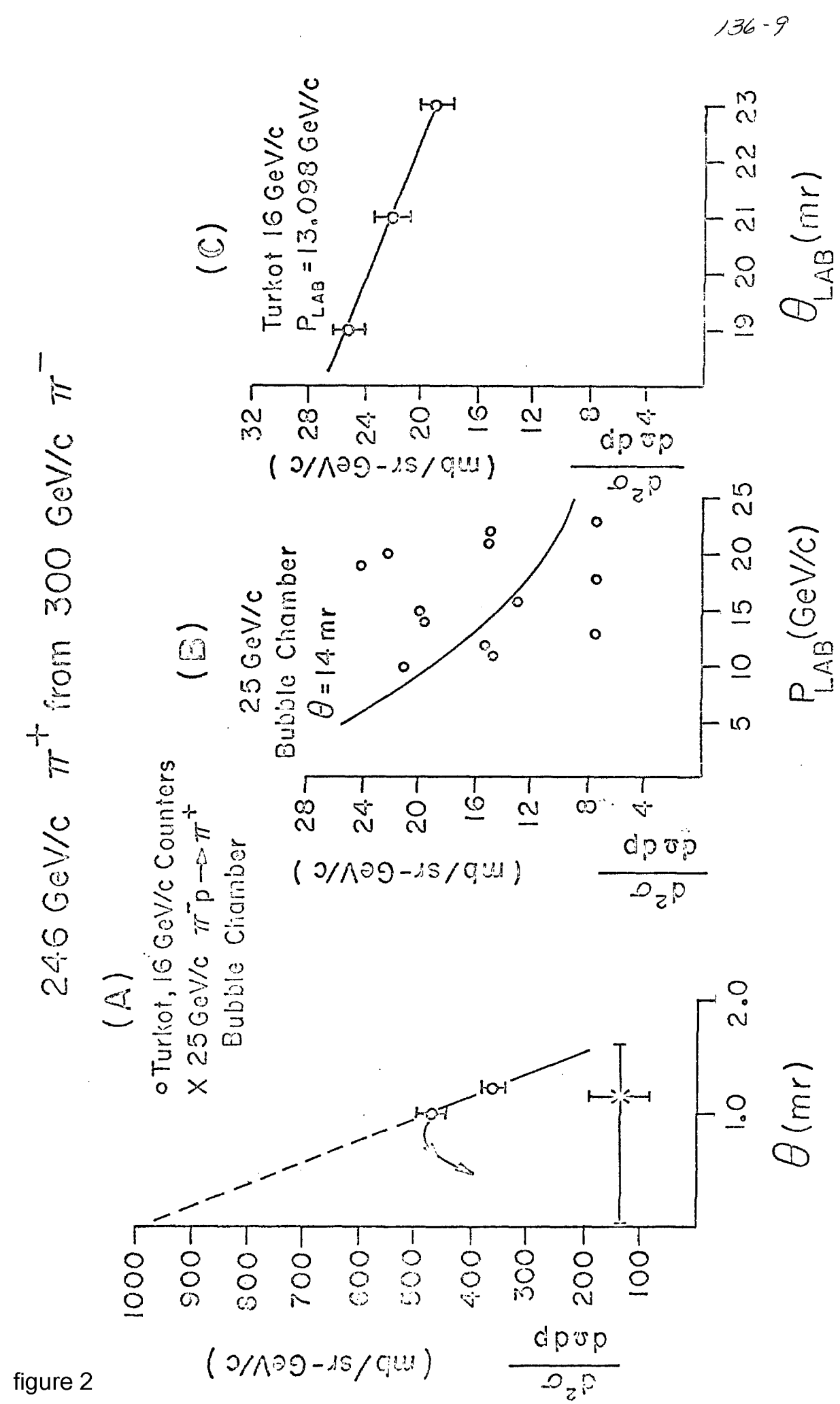
246 GeV/c π^+ from 300 GeV/c π^-
(A)
o Turkot, 16 GeV/c Counters
X 25 GeV/c $\pi^- p \to \pi^+$
Bubble Chamber
$\frac{d^2\sigma}{dpd\Omega}$ (mb/sr-GeV/c)
θ (mr)
(B)
25 GeV/c
Bubble Chamber
θ = 14 mr
$\frac{d^2\sigma}{dpd\Omega}$ (mb/sr-GeV/c)
P_{LAB} (GeV/c)
(C)
Turkot 16 GeV/c
P_{LAB} = 13.098 GeV/c
$\frac{d^2\sigma}{dpd\Omega}$ (mb/sr-GeV/c)
θ_{LAB} (mr)

figure 2

A. Positive Beams

There are two possibilities for positive meson beams which are discussed below:

1. It appears one can obtain a usable π^+ (or K^+) meson flux at 200 GeV/c with essentially no proton contamination. We draw on counter-spectrometer data of Turkot et al.* at 16 GeV/c and our own 25 GeV/c $\pi^- p$ bubble chamber data. High momentum π^+'s are produced by the reaction

$$\pi^- p \longrightarrow \pi^+ + \text{Anything}$$

We make use of the scaling law suggested by Vander Velde** on the basis of limiting fragmentation where the quantity that scales is

$$\frac{1}{p^o} \frac{d^2\sigma}{d\Omega dp} \left(p_T, \frac{p}{p^o} \right) .$$

Figure 2 shows the cross sections expected for 246 GeV/c π^+ production by 300 GeV/c π^-'s. With $\Delta p/p = 1\%$ and 0.25μSR solid angle acceptance this implies between 3 and 9 π^+'s per 10^6 interacting π^-'s on a hydrogen target. A study of our 7 GeV/c π^- data indicates a significant gain in high energy π^+'s when a deuterium target is used, probably because double scattering in deuterium allows a double charge exchange. Ferbel***

---

* Frank Turkot, private communication.

** J. C. Vander Velde, University of Michigan preprint.

*** Tom Ferbel, private communication.

calculates π^+ fluxes from a Be target that are about an order of magnitude larger by assuming reasonable diffractive processes. In this case, however, the proton contamination is unknown but probably small.

If one assumes the usual $\pi^+/K^+ \gtrsim 10$ at the target for zero longitudinal cm momentum ($p_L = 0$), it appears at 25 GeV/c that for large p_L the ratio will be $K^+/\pi^+ \sim 1 - 3$! This is based on a comparison of π^+'s and K^o's produced in 25 GeV/c π^-p interactions.

To use a $\Delta p/p = 1\%$ it will be necessary to know the momentum-dispersed position of the interacting beam particle in order to determine its momentum more precisely. Charpak or wire chambers in front of the bubble chamber will be needed to obtain angular measurements on the incident beam in any case. Tagging the K^+ interactions will, of course, require at least one Cerenkov counter.

2. The simplest π^+ beam can, of course, be obtained using 400 - 500 GeV/c incident protons on a light target and taking 200 GeV/c π^+'s off at a small (0^o) angle. The π^+/p ratio is about 1 in this case, and Cerenkov tagging would produce a useful π^+ beam. We would propose to run in this manner if the double charge exchange feature appears too difficult at turn-on time.

B. Negative Beam

The π^- beam should be the simplest to obtain at 200 GeV/c. Cerenkov counters will not even be needed in this case if the proton momentum is sufficiently close ($\sim$250 GeV/c) to that of the produced π^- beam.

III. DIFFRACTIVE PROCESSES

One of the simplest processes to observe with this chamber will be the diffractive dissociation of the nucleon. We should be able to explore transitions up to masses of 8 → 10 BeV. Thus we should find processes as indicated by the diagram below

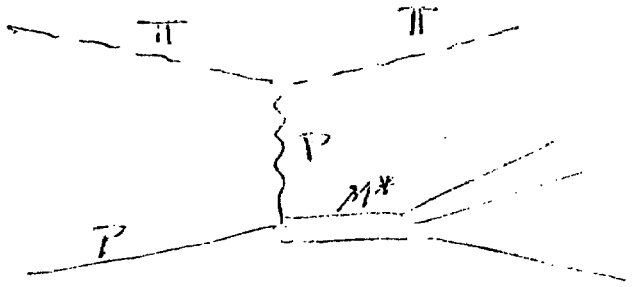

Where M^* is the object which has an I spin of 1/2 and probably has a low spin. Thus we should be able to see such processes as

$$M^{*+} \longrightarrow \rho^0 + P$$

$$\longrightarrow A_2^0 + P$$

$$A_2^- + \Delta^{++}$$

$$\longrightarrow \omega^0 + P$$

$$\longrightarrow P + \bar{P} + P$$

as well as very multiple processes. At present only the simplest diffractive processes have been studied such as

$$M^{*+} \longrightarrow \pi^{+} + N$$

$$\longrightarrow \pi^{+} + \pi^{-} + P$$

$$\longrightarrow \pi^{-} + \Delta^{++}$$

With the higher excitation available it should be possible to observe in a very clean fashion much more complicated diffractively produced objects.

Also, of course, we have the possibility of observing the diffraction dissociation of the incident projectile.

The characteristic of these diffractively produced states is that they show a large enhancement at the threshold for the state. For example, $\pi \longrightarrow \pi + \rho$ shows a peak at a $\pi - \rho$ mass of about 1.1 BeV/c^2. The 5 - π system shows a peak at about 2 BeV/c^2. If the π is really strongly coupled to a quark - anti-quark system then we would expect to see a strongly produced state of mass somewhat greater than 2 M_q. The existence of such a strongly produced mass would be an indication of the existence of such a system even though the quark might be short-lived and have integral charge. A search can be made even though there is no simple signature of the "quark" itself.

IV. *HIGH ENERGY π-π COLLISIONS*

At low energies (~2 BeV) in π^- - P collisions involving one pion exchange constitute a large fraction of the total π^- - P cross-section (7 mb out of a total of 30 mb). At higher energies the fraction seems slightly less but still constitutes a sizeable fraction of the total π - P cross-section. In the 5-10 BeV region simple 2-body processes such as $\pi^- + \pi^+ \longrightarrow \rho^0$ and $\pi^- + \pi^+ \longrightarrow f^0$ are much in evidence (2.5 mb out of 27 mb), and also we see evidence for $\pi^- + \pi^+ \longrightarrow (4\pi)^0$, $\pi^- + \pi^0 \longrightarrow (4\pi)^-$ (probably ~2 mb). These latter processes are difficult to see clearly because they are mixed up kinematically with other processes such as baryonic resonance production. Wisconsin results at 25 BeV indicate that the π - π cross-section seems to become constant at an energy of ~2 BeV and at a value of ~20 mb. The elastic π - π cross-section becomes quite small (1-2 mb) in the 2-3 BeV total energy region. As the bombarding energy is increased it should be possible to observe the inelastic processes associated with the π - π collisions. For example, we might expect to find a) $\pi^- + \pi^- \longrightarrow (3\pi)^- + \pi^-$ (by looking at reactions $\pi^- P \longrightarrow \pi^- + \pi^- + \pi^+ + \pi^- + \Delta^{++}$) or b) $\pi^- + \pi^0 \longrightarrow \rho^- + \rho^0$. $\pi^- P \rightarrow (\rho^- \rho^0 P)$

The thing easily observable in these reactions is the recoiling baryon (either at Δ^{++} in reaction a) or a recoiling nucleon in reaction b).

In the 100 - 200 BeV range for the π the products of the π-π collision tend to be moving with several BeV with respect to the nucleon. This means that the kinematic mixing which occurred at lower energies should not be a problem. The difficulty in observing the reactions has to do with establishing the G parity of the pion combinations.

The biggest contamination will come from diffractive dissociation of the π. For example, we need to differentiate between

$$\pi^- + P \longrightarrow \pi^- + \pi^- + \pi^+ + \pi^o + P$$

and

$$\pi^- + P \longrightarrow \pi^- + \pi^- + \pi^+ + P \ .$$

Both of these reactions tend to occur with a small momentum transfer to the nucleon. If the π^o has a momentum of 10 BeV/c or greater it should be relatively easy to detect. Thus at least in a considerable fraction of the events of type c we should be able to differentiate c) from d). We observe a cross-section of about 0.8 mb for each of these reactions at 25 BeV.

What Can Be Done with Limited Facilities?

We can look at events with recoiling protons. For such events one can calculate the missing mass. For low missing mass (1-2 BeV) this can be done only crudely but by 2 - 4 BeV the missing mass may be measured with modest precision ($\sim \pm$ 1 BeV). By counting with some γ-

detection capability we can determine whether there are an even or an odd number of π's present (assuming that all the emerging fast particles are π's).

For a given even G parity state in a given mass range we can look at the momentum transfer spectrum of the recoiling nucleons on Δ^{++}, to see if it is characteristic of one pion exchange. There are other checks that one can make to see if the OPE process makes any sense. For example, fore aft symmetry in the dipion rest frame would be a check that one could make. We believe it is possible to look at $\pi^- - \pi$ collisions without analyzing the events in detail. We can also cross check the results by comparing $\pi^+ + n \longrightarrow (4\pi \text{ or } 6\pi)^o + p$ with $\pi^+ + p \longrightarrow (4\pi \text{ or } 6\pi)^o + \Delta^{++}$.

V. QUARK SEARCH

Considerable effort has been devoted to the search for quarks both at accelerator and cosmic ray energies. So far all of the direct efforts have failed to find any such objects. It is conceivable that quarks have integral charge and are very shortlived. In such a situation one might expect no particular signature. The only clue might be an enhancement in a mass spectrum. For example, consider the pion.

$$\pi^- \Rightarrow q\bar{q}$$

so that

$$\pi^- p \longrightarrow (q\bar{q}) + p$$

in a diffractive fashion. We would then expect to see an enhancement which rises beyond $2 M_q$ in the mass spectrum of the produced object. The free quark state might show only as an enhancement in the 7 or 9 pion state produced diffractively. An analogous situation would seem to be in the process $\pi^- \longrightarrow \bar{p}n$. The diffractive process seems to have a cross-section of $\sim$10 - 20 ub whereas one also observes a peak in the 5π spectrum in the mass range of 2 BeV which may reflect this same $\bar{p}n$ state. The 5π cross section is probably larger than the $\bar{p}n$ production by an order of magnitude.

For 200 BeV pions we can effectively explore the diffractively produced mass range of 1 $\longrightarrow$ 9 BeV. Thus we might expect to explore up to quark masses of 3 - 4 BeV. We could also see quark pairs produced in $\pi - \pi$ collisions up to a similar mass range.

By having π^+-d, π^--p, π^+-p one has the possibility of looking at both neutral and charged states for an enhancement in the same mass range.

VI. γ-RAY DETECTION AND TRIGGERING

We propose to detect γ-rays from fast π^o's and to measure their positions in the wide-gap chamber by placing 1/2" lead plates between the two downstream wide-gap spark chambers. A 3" wide by 7" high hole will permit the beam to pass through without scattering. About 85 percent of the γ-ray passing through the lead plate will convert and produce a pulse in one of the scintillators covering the full area of the lead and also provide visible tracks in the chambers which will permit a measurement of the γ-ray direction. A second similar set of plates and counters will be placed between the upstream chambers to cover a part of the area of the exit port in the magnet that is not covered by the downstream spark chamber, as viewed from the target region of the chamber. In addition to the triggers discussed in the Appendix, we will also trigger on a coincidence between a beam-particle and any of the γ-ray counters. This will reduce the inefficiency for those cases of a single forward-going charged particle which happens to pass through the beam counter.

Downstream of the trigger and coincidence counters we will place a further γ-ray detector to detect π^o γ-rays which pass through the 7" x 3" hole in the lead in the downstream spark chambers. This detector will consist of a plate of lead 1" x 48" x 20" with four 24" x 10" scintillation counters covering its back furface. The pulse from the four counters will be added, analyzed and recorded when in coincidence with the trigger pulse.

There will frequently be a charge particle passing through this counter but the number will be known from the spark chamber data and the pulse from a shower developed in four radiation lengths of lead will be clearly distinguishable from charge particles unaccompanied by γ-rays.

Thus fast π^o's will be detected over all the forward solid angle with high efficiency. This will identify events with a fast forward π^o and will be very useful. A very common final state comes from

$$\pi^- p \rightarrow \pi^- + \pi^o + \pi^o + p$$

where the π's come from diffraction dissociation of the π^-.

Importance of γ-Ray Detection

It is obviously very important to detect γ-rays for both physics and technical reasons. Physics-wise it is important to know the number of π^o's to determine the G-parity of a given state.

Technically the information on the presence or non-presence of π^o's will be of enormous help in fitting of events in a situation of marginal momentum determination. As a simple example, suppose we have an event which might look as below

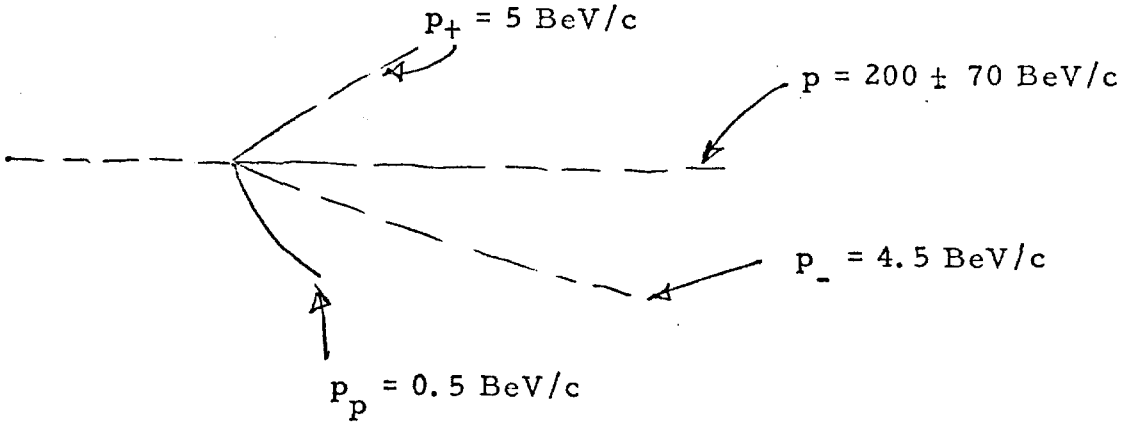

The transverse momentum balance for the slower tracks might be to within ± 50 MeV/c. The thing that one does not know is the momentum of the forward going particle. If it has a momentum of 130 BeV/c then there are likely to be 1 or more π^o's in a very small cone about the outgoing fast π. The knowledge that there are no π^o's present will allow one to fit the event with accuracy a sizeable fraction of the time. One can generalize this to a more complicated final state as well.

If both γ's from a π^o are detected, one can determine the momentum of the π^o to modest precision (~~5-10~~ 10-50 percent) by measuring the opening angles.

IV. Experimental Arrangement for the Proposed 30-inch Bubble Chamber - Optical Spark Chamber Hybrid System

The main components of the proposed detector system are shown in Figure 1. These include:

(1) The 30-inch hydrogen bubble chamber, for observation of the interaction vertex and analysis of all low energy charged particles with momenta below ~20 GeV/c.

(2) An upstream beam diagnostic system for providing precise measurements of beam particles.

(3) A wide gap optical spark chamber spectrometer situated downstream for providing important additional data on energetic secondary charged particles with momenta above approximately 20 GeV/c.

(4) A shower spark chamber system situated behind the spectrometer for information on very energetic gamma rays.

While the arrangement is similar in some respects to the bubble chamber - spark chamber detector system described in the Aspen study of Fields, et al.[1], it is not required for the present initial experiment to have the very high accuracy requirements for final state fitting which was of primary interest in the latter study.

These components are matched to the kinematic requirements, as discussed below, in such a way that they provide relatively complete examination of individual multiparticle interactions in the 100 GeV/c region and above. The most noticeable feature of multiparticle interactions as presently known is the tendency for the emitted particles to be produced with relatively small transverse momenta. Those going backwards in the cm system with large longi-

tudinal momenta then appear in the laboratory system with low momenta and large angles. Particles with small longitudinal momenta can appear in the lab at intermediate momenta and angles, while the forward particles in the cm appear as highly collimated, energetic components of a forward jet.

Examples of kinematically allowed regions for transverse and longitudinal cm momenta are shown in the Peyrou plot of Figure 2 for the case of 500 GeV/c pp interactions. Superposed are the expected contours for laboratory angles and momenta of outgoing pions, showing the characteristics described above. For greater detail, the region of small transverse momenta is shown in Figure 3. Backward pions in the cm with transverse momenta below 1 GeV/c are seen to have laboratory momenta of less than $\sim$20 GeV/c, and can appear at angles even beyond 90°.

Similar behavior is illustrated for secondary protons from 200 GeV/c pp interactions in Figure 4, except that the allowed maximum laboratory angle here must be less than 90°. On the other hand, those particles produced with small or forward longitudinal momenta P_L, and transverse momenta $P_T \lesssim 1$ GeV/c, are seen to have laboratory momenta above approximately 20 GeV/c and are confined to a forward cone of less than approximately ±4° opening angle.

A. Bubble Chamber

The main bubble chamber requirements here are good track resolution, angular precision $\lesssim$ 1 mrad, good momentum accuracy up to the 20 GeV/c region, and provision of suitable exit windows and magnet apertures for the forward secondaries. The 30-inch bubble chamber is eminently suitable, without requiring any significant modifications.

The gross chamber features illustrated in Figure 1 are those of the 30-inch, whose characteristics include high resolution dark field optics, a

magnetic field of 32 Kg, multipulsing capabilities of $\leq$ five expansions per 0.5 seconds, and a maximum detectable momentum of over 1000 GeV/c. In the configuration shown in Figure 1, the beam is brought in through a small window which is currently in use as an exit window for a neutral hadron hybrid spectrometer at ANL. The limiting exit angle allowed by the magnet structure in the horizontal plane is confined to approximately ±3.5°, which corresponds to allowing all secondary particles above ~20 GeV/c to enter the downstream spark chamber spectrometer. In the vertical plane the magnet iron and beam exit windows allow particles at angles up to approximately ±10°. Thus, it is obvious that the analysis of tracks below ~20 GeV/c will necessarily be performed in the bubble chamber, where $\Delta p/p \leq 10\%$ and $\Delta\theta \leq 1$ mrad. This, in our opinion, is a satisfactory level of performance for this particular group of produced particles.

B. Bubble Chamber Beam

Since the spectrometer facility is planned to be of general use, a comprehensive beam system is required. This section discusses beam characteristics and beam defining equipment which we regard as necessary to do a variety of experiments in the 30-inch bubble chamber with the associated downstream spectrometer. It is assumed that the beam, as described in the Lach-Pruss report[2], will be constructed, including a secondary hadron target. It is also assumed that fluxes of at least 10^{10} protons will be available at the secondary hadron target, with a spill time between 60 and 200 μ sec. Two or three such spills per accelerator pulse would be highly desirable for bubble chamber multi-pulsing. In addition, it is assumed that beam tuning detectors (scintillators or wire proportional chambers) will exist, and also at least one Cerenkov counter to determine relative fractions of π, K and p.

In addition,

A) it is felt that a flux-limiting fast kicker will permit much more efficient use of the bubble chamber, giving cleaner pictures and avoiding unusable pictures;

B) a Cerenkov counter which can efficiently tag π's vs. (K and p) up to 200 GeV/c is desirable for beam purity in view of possible significant fractions of K^- and $\bar{p}$[2,3];

C) a second Cerenkov counter which can tag (π^-, K^-) vs. $\bar{p}$ will permit studies of K^- and $\bar{p}$ interactions as a by-product of a π^- experiment. Eventually K^- and $\bar{p}$ enrichment triggering might be done. If K^+/p and π^+/p ratios are good, similar arguments will apply for positive beams;

D) position tagging of each beam track in the chamber, in time correlation with the above Cerenkov signals, will be necessary.

E) external determination of beam momentum and angles will be mandatory in most cases. Five small proportional wire chambers can do this job and also tag all beam tracks in (D).

We now discuss items (A) - (E) in greater detail.

A) Fast Flux limiting Beam Kicker

A 1-2 μ sec. kicker with integral $Bdl \cong$ one Kg-m would kick the 5mm high target image upward by 0.065 mrad, or by 13 mm with a 200 meter lever arm. The kicker should be located 1000 feet from the chamber. However, the beam track counter should be placed at the chamber entry window to avoid uncertainty in n. The signal propagation delay ($\sim$2 μ sec.) is comparable to the rise time, plus there are logic and ignition delays. Given a total delay of 4 to 7 μ sec., n = 10 tracks/picture, and 100 μ sec. spill time, one could control the flux to 10%, which is excellent. This is enormously better than

the typical fluctuations without a kicker, and should eliminate a source of wasted bubble chamber photographs and wasted accelerator pulses.

B and C) Cerenkov Tagging of π, K and p

Extrapolations[3] of Serpukhov data indicate that 500 GeV/c protons on a target will produce a rich ratio of K^-/π^- and $\bar{p}/\pi^-$ at 100 GeV/c -- 5% and 15% respectively, 1 km. away at the bubble chamber. The need for π^- tagging in this case is obvious, and the opportunity to study tagged K^- and $\bar{p}$ interactions early is attractive. In secondary positive beams, p and π^+ and probably K^+ will all be present in significant amounts at some energies, and will require tagging.

S. Pruss (NAL) has suggested a differential Cerenkov design, an outgrowth of ideas he presented at the 1970 Summer Study[4]. Small angle light is directed to one phototube and light between this angle and a larger angle is directed to a second phototube. For Cerenkov angles $\sim$5 mrad, the angular separation of π's from K's at 200 GeV/c is several times the natural beam divergence of 10^{-4}mrad, or the chromatic $\Delta\theta$. Good photon fluxes at these angles should permit efficient tagging at $p \lesssim$ 200-250 GeV/c or beyond. A second Cerenkov counter of identical design would then permit separation of p from K and π.

The design involves 40m of Helium-filled pipe at $\sim$.2 to 1 atmosphere absolute, downstream diameter 12" to 18", a 100" focal length spherical mirror, and the above-mentioned phototube array. High counting efficiencies can be obtained even beyond 200 GeV/c in the differential mode of operation with this length. Beam divergence must be $\lesssim$ 0.1 mrad, close to what is achievable in the existing beam design.[2] Pressure must be monitored to 10 mm of mercury and average temperatures to 5°C.

D) Position Tagging of Tracks to Correlate with Cerenkov Information

Minimal position tagging could be accomplished with a crossed pair of picket fence scintillator arrays. This means a non-negligible number of photomultiplier tubes, since the number, m, of x-y resolution elements should be many times greater than the number, n, of beam tracks to reduce the probability of two tracks in one hodoscope location. Moreover, one must record the bubble chamber frame number and x-y for each beam track. Thus, a fast parallel shift register is needed to absorb information during the beam spill and later pass it on to a computer or perhaps directly to an incremental tape unit.

With this in mind, we suggest the use of small proportional wire arrays of 50 to 100 wires, read out as above. One gets greater x-y resolution at somewhat less cost and can also achieve the purposes of item (E). Such a system is illustrated in Figure 5.

E) Angle and Momentum Tagging.

To use the 30" bubble chamber efficiently, one should start the fiducial volume immediately at the beginning of the liquid. Hence, one must know p and θ of the beam externally. In any case, one can do better externally than by measuring short beam tracks in the liquid. From beam optics one will have $\delta\theta \simeq 10^{-4}$ rad and $\delta p/p = 0.066\%$.[2] However, in flux-limited situations one may want to increase the momentum bite to 1%. Then it pays to replace the momentum slit with a proportional wire array and win back the $\delta p/p$ inherent in the target size. This corresponds to a wire spacing of 2mm. A more refined system can be made with 1 mm. wire spacing, but several such chambers would be required to determine orbits better. In effect, the equivalent of a second plane near the target is needed to reduce the "target size". In

this case one also improves upon the .066% which can be achieved with momentum slits.

The phase space of the beam as designed is 10^{-9} inch^2-steradian. With a reasonable beam size in the chamber, for example $\sim$ 0.5 x 3.0 inches, either the beam is parallel to 10^{-4} rad or its angle can be determined to 10^{-4} by measuring position in the chambers. This matches $\delta\theta_{coulomb} \leq 10^{-4}$ from the entry windows, and also matches for beam up to 500 GeV/c with the transverse momentum accuracy one obtains from measuring outgoing tracks in the last half of the bubble chamber or better still in the wide gap optical chambers.

To survey the proportional chambers, a well measured non-interacting track in the bubble chamber determines θ to 0.5×10^{-4} in y, and 1.5×10^{-4} in z, while $\delta\theta(\text{coulomb}) \sim 10^{-4}$ from the entry windows. At a distance of 13 m, the wire location is known to 1.5 and 2.4 mm respectively in y and z, from a single track.

We propose to use an existing, tested design of Charpak chamber[5] with good space resolution and immunity to spark chamber noise, compact and with a relatively small number of wires in total. We could certainly put the information onto magnetic tape, together with Cerenkov counter signals, for each beam track into the bubble chamber. Frame numbers would also be written onto the tape between beam pulses. A small computer would be the most flexible readout device. A fast parallel shift register or equivalent will be needed to interface the proportional wire and Cerenkov signals. The computer could in principle be dispensed with and the information written directly from the shift register by an incremental tape unit, but with the loss of online diagnostic capabilities. Given a computer with a fast printer, the track tagging information could be printed out frame by frame for each roll,

avoiding magnetic tape and associated format problems for the users.

C. Spark Chamber Spectrometer

Although many of the salient features of multiparticle interactions will be obtained from the analysis of only the low energy particles seen in the bubble chamber, as illustrated in the previous discussion, we believe that additional insight can be provided by supplementary information on the more energetic downstream components of the same events. The following deals with four important aspects of the system:

(A) spectrometer resolution,

(B) spark chamber optics,

(C) gamma-ray detection and,

(D) trigger schemes.

(A) Spark Chamber Spectrometer Resolution

The apparatus, as shown in Figure 1, includes no external magnetic field other than that of the bubble chamber itself. Calculations show that utilizing (a) the event vertex location in the bubble chamber (b) the chamber's fringing field and (c) track locations in the wide gap chambers a typical $\Delta p/p$ accuracy of ±5-10% or less is readily obtainable for fast secondaries produced in a 200 GeV/c collision on hydrogen. It is clear, however, that considerable additional accuracy is available on the very small angle fast secondaries with the addition of a magnet downstream. Preliminary considerations for such a system are also presented.

In the initial scheme, two spark chamber units are utilized, one immediately behind the bubble chamber magnet with four gaps of active volume 36" wide by 48" high by 8" deep and the other unit 4.5 meters downstream, against

the far wall of the bubble chamber building, with the same dimensions. The downstream 36" dimension subtends a ±3.5° angle from the bubble chamber. Assuming the following perameters: (1) ±500 μ on each point measured in the spark chambers (2) eight points measured per spark chamber unit (3) ±50 μ on the vertex in the bubble chamber and (4) 872 Kg-in of integral Bdl in the bubble chamber fringing field we find that $\pm\Delta p/p$ (%) $\tilde{-}$ 0.07 p (GeV/c). Taking into account the following sources of error due to multiple coulomb scattering: (1) 15" of LH_2 (2) 0.12" of Fe (B.C. window) (3) 0.25" of Al (vacuum tank windows) and (4) 0.5 cm of counters and other smaller sources (air, chamber walls), the resultant $\pm\Delta p/p(\%)$ has been determined and is shown in Figure 6. With the exception of the fastest secondaries produced at the highest momenta proposed, the calculations show that the downstream spectrometer will provide data comparable in accuracy to that of the bubble chamber at lower secondary momenta and permit a complete study, in conjunction with the bubble chamber, of all interesting production angles.

The necessary and straight forward extension of the apparatus to yield more precision in the momentum determination of fast forward particles requires an additional spark chamber module plus a magnet. This would involve a large aperature magnet (e.g., an ANL type BM 109 with a 8" x 24" x 72" aperature and maximum integral Bdl of 1366 Kg-in) placed immediately downstream of the second spark chamber module followed by a third spark chamber module 5 meters from the magnet. All tracks with lab momentum $\gtrsim$ 100 GeV/c and with transverse momentum $\lesssim$ 1 GeV/c will be transmitted through the aperature of the magnet and will be recorded in the third spark chamber module. The deflection in the magnet, coupled with the long lever arm, provides a $\pm\Delta p/p \lesssim .012\ p\ (\%)$. Thus, 6-7% $\pm\Delta p/p$ or less can be achieved for all tracks of interest without altering the initial setup of the experiment.

(B) Spark Chamber Optics

The wide gap chambers have an active volume 8" deep x 48" high x 36" wide per cell. Each chamber consists of 2 cells and each module consists of 2 chambers, as seen in Figure 7. The chambers are mounted on a precision platform which has three primary functions: 1) Providing a means of determining the relative locations of the two chamber modules and the bubble chamber, 2) Providing a means of maintaining a continuous check on these positions and 3) Providing a simple means of re-installing the apparatus in the beam line after removal. Measuring of apparatus locations is done by means of two theadolites, one to determine and monitor bubble chamber-spark chamber platform positions and the second to determine and monitor spark chamber-spark chamber platform positions. Leveling legs on the chambers, top, bottom, front, and rear fiducials on the chamber frame and fiducials on the precision platform serve to position the chambers in a known orientation. Front and top fiducials also appear on each film frame to orient the chambers on the film. Rear and bottom fiducials on periodically run fiducial runs serve to complete a three dimensional co-ordinate system for track reconstruction independent of knowledge of camera position. Additional platform fiducials in view of the camera can serve as an extra check on spark chamber-platform orientations.

The chamber separation is variable within and between modules. Within the module a maximum separation of 32" is allowed. As seen in Figure 8, this maximum separation still permits viewing both chambers in a module with one 35 mm. camera at a demagnification of 64:1. This demagnification is an upper limit permitted by the intrinsic resolution of a film such as Kodak Shellburst for a real space position accuracy of 0.1 mm. With a 4" lens

the camera can be located at 20 ft. from the center of the chambers. The chambers are inclined 6° relative to the beam line to permit a direct view in each chamber, thereby eliminating lenses and mirrors in that view (see Figure 9). The chamber windows are made of 10 mil. clear Mylar to eliminate distortions there. One precision mirror is used in the 90° stereo view to bring that view to the same camera. A fiducial plane with many fiducials is located at the bottom of the spark chamber to permit corrections due to any distortions in the mirror. 90° stereo is used for maximum accuracy in reconstruction. The direct view is the view of the plane of bend for maximum accuracy in momentum determination. A strip mirror subtending $\sim 1/3$ of the gap in the direct view provides 10° stereo for resolving ambiguities in track reconstruction. The mirror subtends only part of one gap in each chamber to eliminate confusion between the direct and 10° stereo tracks. A dark room under slight over pressure surrounds each assembly for photographic and hydrogen safety reasons.

(C) Gamma-Ray Detection

The insertion of several radiation lengths of material between the second and third gaps of the spark chamber units will provide an effective converter for gamma-rays from fast, forward π^0's. From the point of interaction, probably measureable to $\lesssim$ 5 mm, both the frequency and direction of fast π^0's can be inferred. To our knowledge, the only previous measurement of π^0 frequency is that of Elbert et al.[6] at 25 GeV/c for π^-p in a hydrogen bubble chamber with plates. Their results, although somewhat weak statistically, are in rather strong disagreement with the multiperipheral model. Clearly, more precise measurements at NAL energies will be very valuable in our proposed studies.

(D) Trigger Schemes

The trigger arrangement will be designed such that the spark chambers fire on virtually all interactions, there being nearly one per beam burst. A picture of the bubble chamber will be taken for each expansion. Two simple and flexible schemes have been devised:

(1) Energy-Loss Trigger: Referring to Figure 1, multiparticle-charge-particle secondaries would be selected by pulse-height criteria in the counters S_3 S_4 S_5. More than one particle will, on the average, give a greater pulse height than that for a single beam particle. Although one might consider almost any type of counter which gives signals proportional to the number of particles which transverse it, e.g. Cerenkov, scintillation, etc., the most simple to utilize is the scintillation counter and it also turns out to result in the thinnest detector (in g/cm^2). A single scintillation counter when traversed by a high energy particle will give a Landau pulse-height distribution. This distribution, with its long tail at high pulse heights, cannot be avoided in the present application. A pulse height of 2 times the minimum value will occur on traversal by a single minimum ionizing particle ~5% of the time. This can be greatly improved, however, if two or more counters S_1, S_2; S_3 S_4...S_n are utilized and the minimum pulse height appearing is considered. In this case, the width of the distribution will be decreased by $1/\sqrt{n}$ and even for $n = 3$, the tail has all but vanished. If this signal is to be used to trigger the downstream chambers, the minimum pulse height must be determined in $<<1$ μ sec.

With this method, it is to be noted that the downstream counters should be thin in order that nuclear interactions in them do not occur frequently. Such interactions are no different in character from those in the chamber and

walls and triggers due to them would certainly result. The number of these should be much smaller than those which occur in the chamber. In 1 mm of plastic scintillator a minimum ionizing particle produces $\sim 10^3$ photons. With an efficient photo cathode ($\sim$25%) and a light collection efficiency of $\sim$20%, 50 photo-electrons could result. This number is sufficient to assure that statistical fluxtuations will be relatively small. The five counters, S_1, S_2, S_3, S_4, and S_5, would represent a total thickness of 0.5 cm which is 0.5cm/52cm = 1/100 of a geometrical-mean-free-path. Thus, with 6 particles per picture and with the counters described, in $\sim$ 6% of the pulses would the spark chamber system have recorded interactions occuring in the triggering counters $S_1S_2S_3S_4$and S_5.

For reasons of efficient and uniform light collection the size of these counters probably should not exceed 8" x 8". This presents some minor limitations in the detection of secondaries as they must appear within a cone of ±3° if placed at a distance of $\sim$2 meters from the interaction. It may be possible to locate counters nearer the chamber inside the iron yoke, and if so the acceptance angle would be increased. This setup is very inefficient for elastic scattering and processes of the type $pp \rightarrow ppn(\pi^\circ)$, when the struck proton is slow and at a large angle, thus missing $S_3S_4S_5$. However, an alternate scheme, discussed next, would resolve this shortcoming. Also, with this arrangment one also might consider triggering on events with no charged secondary within the angular acceptance of $S_3S_4$and S_5. This alternate trigger could be tried with parallel logic and could be easily included or not as a parallel trigger.

(2) Beam-Deflection Trigger: The trigger consists of a 3.0 inch diameter scintillator S_3 located in the beam 125 feet downstream from the

bubble chamber (see Figure 1). When this scintillator fails to record a particle previously observed by counters S_1, S_2 in the beam upstream of the bubble chamber, it is considered to have interacted.

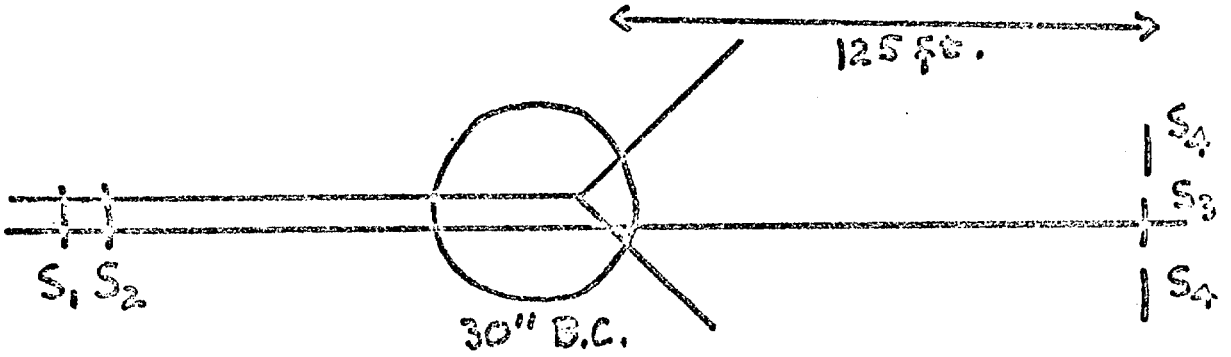

For the purposes of investigating the properties of the trigger we assume a 2.0" diameter beam in the bubble chamber. This allows a beam spread which does not diverge after leaving the chamber except for multiple Coulomb scattering. For beam momenta between 100 and 500 GeV/c the beam size at the downstream scintillator should not exceed 2.25 inches due to multiple scattering.

This trigger fails most frequently in detecting elastic scatters. Table II below lists the average minimum scatter angle and recoil range for elastic events which will actuate the trigger.

TABLE II - Minimum Angle and Recoil Range For Elastic Events

Beam Momentum GeV/c	Minimum Scatter Angle mr.	Minimum Recoil Range cm
100	1	0.3
200	1	3.5
300	1	15.0
500	1	100

There is considerable flexibility here. For example, by moving S_3 to 200 feet downstream of the bubble chamber and using a diameter of 2.5"

instead of 3.0", one achieves a minimum angle of 0.5 mr. and a minimum range of 8.0 cm at 500 GeV/c.

Some fraction of the inelastic events might also be expected to put a particle through S_3, invalidating the trigger. Scaling 25 GeV/c events to NAL energies indicates this is not very important, in part because the bubble chamber field imparts transverse momentum to a track which is several times that of the minimum detectable elastic scatter. For example at 200 GeV/c this trigger fails on 4.5% of the 2-prongs, 3% of the 4-prongs, 1% of the 6-prongs and 0.3% of the 8-prongs.

This small loss of inelastic events can be reduced somewhat by surrounding S_3 with a larger counter S_4. A hole in S_4 passes beam particles on to S_3. A multiparticle accidental through S_3 is likely to be accompanied by one or more particles through S_4. Hence one would trigger on $(S_1.S_2.\overline{S_3}.S_4)$, $(S_1.S_2.\overline{S_3}.\overline{S_4})$, $(S_1.S_2.S_3.S_4)$. One can reduce the loss rate arbitrarily by increasing the size of S_4 or moving it closer to the bubble chamber.

S_3 was not placed more than 125 feet downstream of the bubble chamber so that transit time of the particles and signals would be short enough to allow adequate time to perform logical operations and apply spark chamber voltages in less than 500 ns. This restriction is probably too strict by at least a factor of two and can probably be relaxed to observe smaller angle elastic scatters. Some groups will probably prefer a beam profile in the chamber more like 5" x 1/2". In this case S_3 would be about 6.5" x 1". This has approximately the same solid angle as the circular counter discussed above and presents no focusing problems for the presently planned beam.

Finally, it is emphasized that both these triggers are flexible and most certainly can be studied quickly and efficiently under test beam condi-

tions. It would be our intention to do so before proceeding with "production" data-taking.

REFERENCES

1. T. H. Fields, et al., NAL Summer Study, Vol. 3, 227 (1968).
2. "Hadron Beams in the Neutrino Area", J. Lach and S. Pruss, NAL Report TM-285, 2254.000.
3. "Extrapolated Ratios of K^- and $\bar{p}$ to π^- from High Energy Protons on Aluminum measured at Serpukhov," V. E. Barnes, Purdue University High Energy Physics Note # 313, April 1, 1971.
4. S. Pruss, NAL Summer Study (1970) p. 103.
5. M. Atac and J. Lach, Nucl. Instr. & Methods 86, (1970) p. 173.
6. J. W. Elbert et al., Nuclear Physics B19, 85 (1970).

FIGURE CAPTIONS

Fig. 1 Components of the proposed hybrid system.

Fig. 2 Contours of laboratory angle and momentum on the Peyrou Plot for the π in the reaction $p + p \rightarrow \pi^+ + \ldots$ at 500 GeV/c.

Fig. 3 Shows more detail of Fig. 2.

Fig. 4 Detail of contours of laboratory angle and momentum on the Peyrou Plot for the proton in the reaction $p + p \rightarrow p + \ldots$ at 200 GeV/c.

Fig. 5 Upstream proportional wire spectrometer.

Fig. 6 Calculated momentum resolution for the apparatus of Fig. 1.

Fig. 7 Wide gap optical spark chamber (one of two such chambers).

Fig. 8 Wide gap optical spark chambers and camera positioning.

Fig. 9 Format of images on 35 mm film.

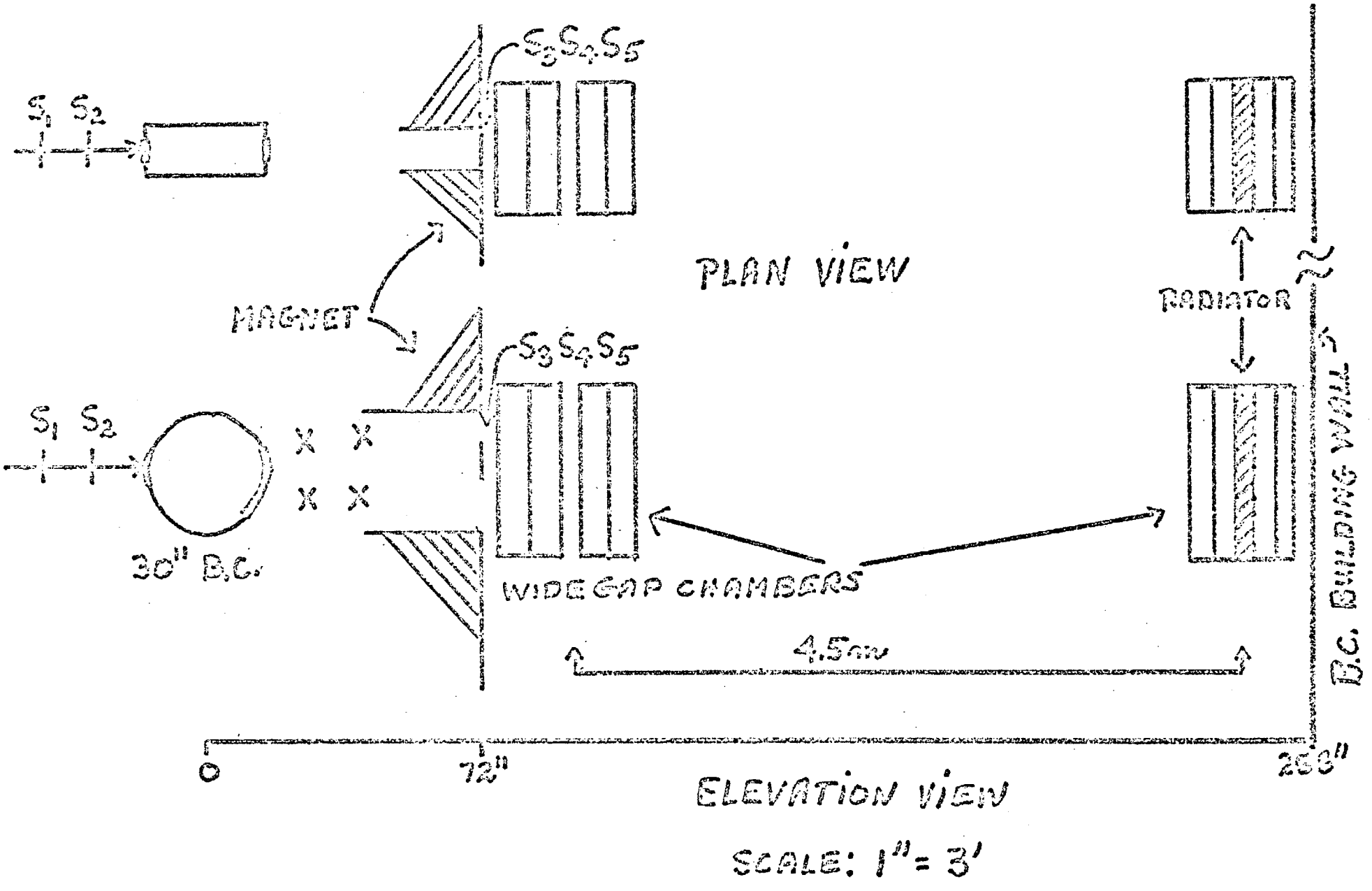
S1 S2
S3 S4 S5
MAGNET
PLAN VIEW
RADIATOR
B.C. BUILDING WALL
30" B.C.
WIDE GAP CHAMBERS
4.5m
0
72"
288"
ELEVATION VIEW
SCALE: 1" = 3'

14-81

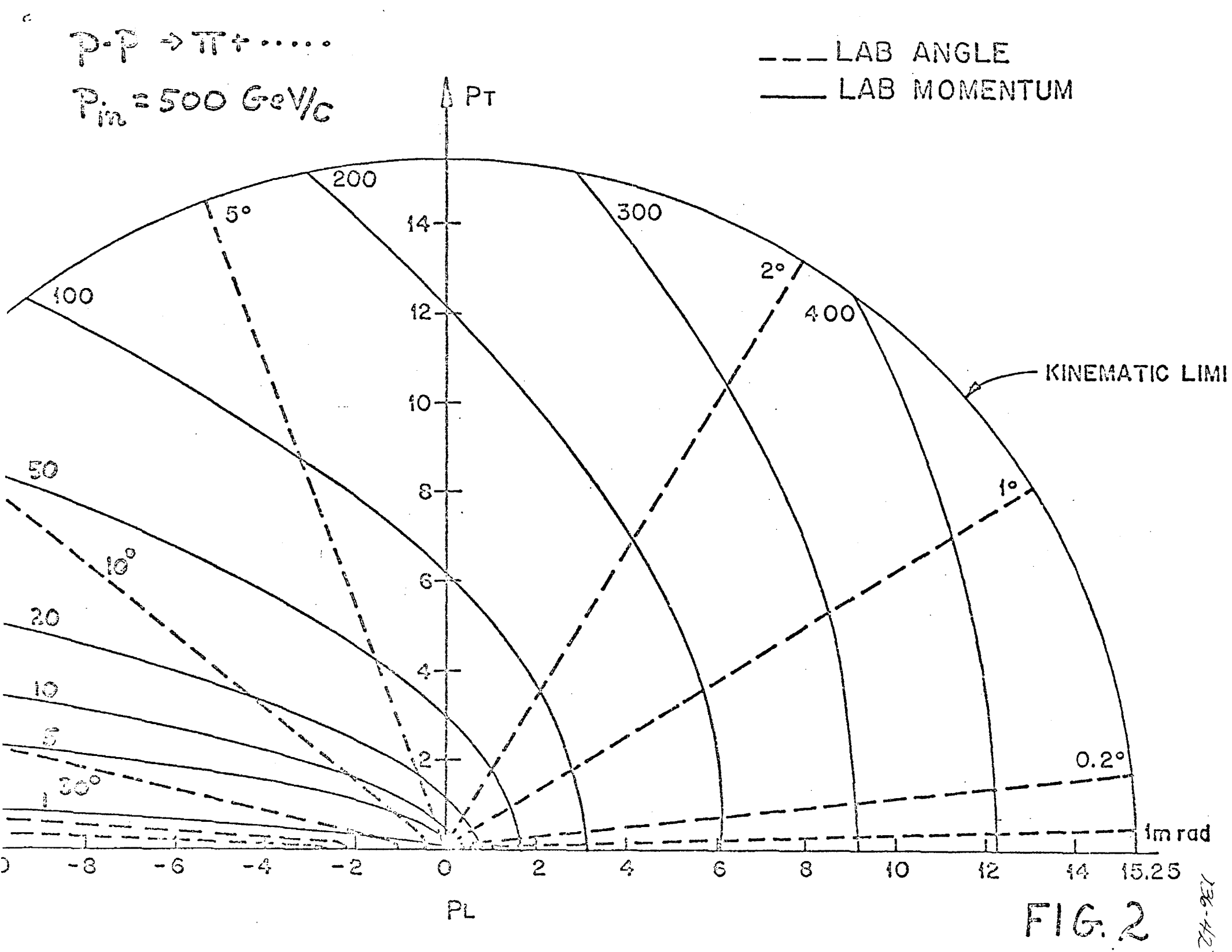
p-p → π+ ....
P_lm = 500 GeV/c
--- LAB ANGLE
—— LAB MOMENTUM
PT
PL
100
200
300
400
50
20
10
5
1
5°
2°
1°
0.2°
30°
10°
1m rad
KINEMATIC LIMI
14
12
10
8
6
4
2
0
-8
-6
-4
-2
2
4
6
8
10
12
14
15.25

FIG. 2

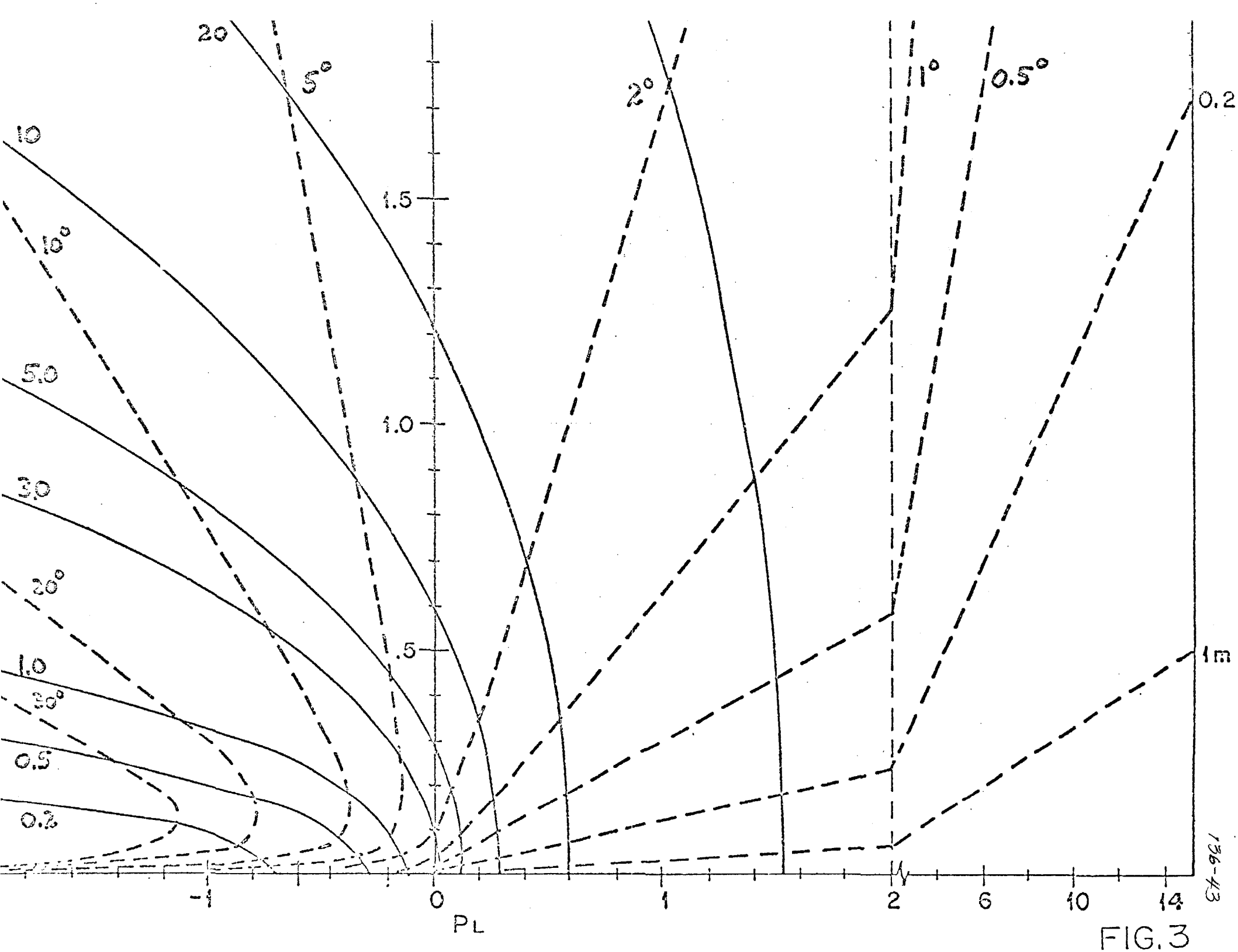

FIG. 3

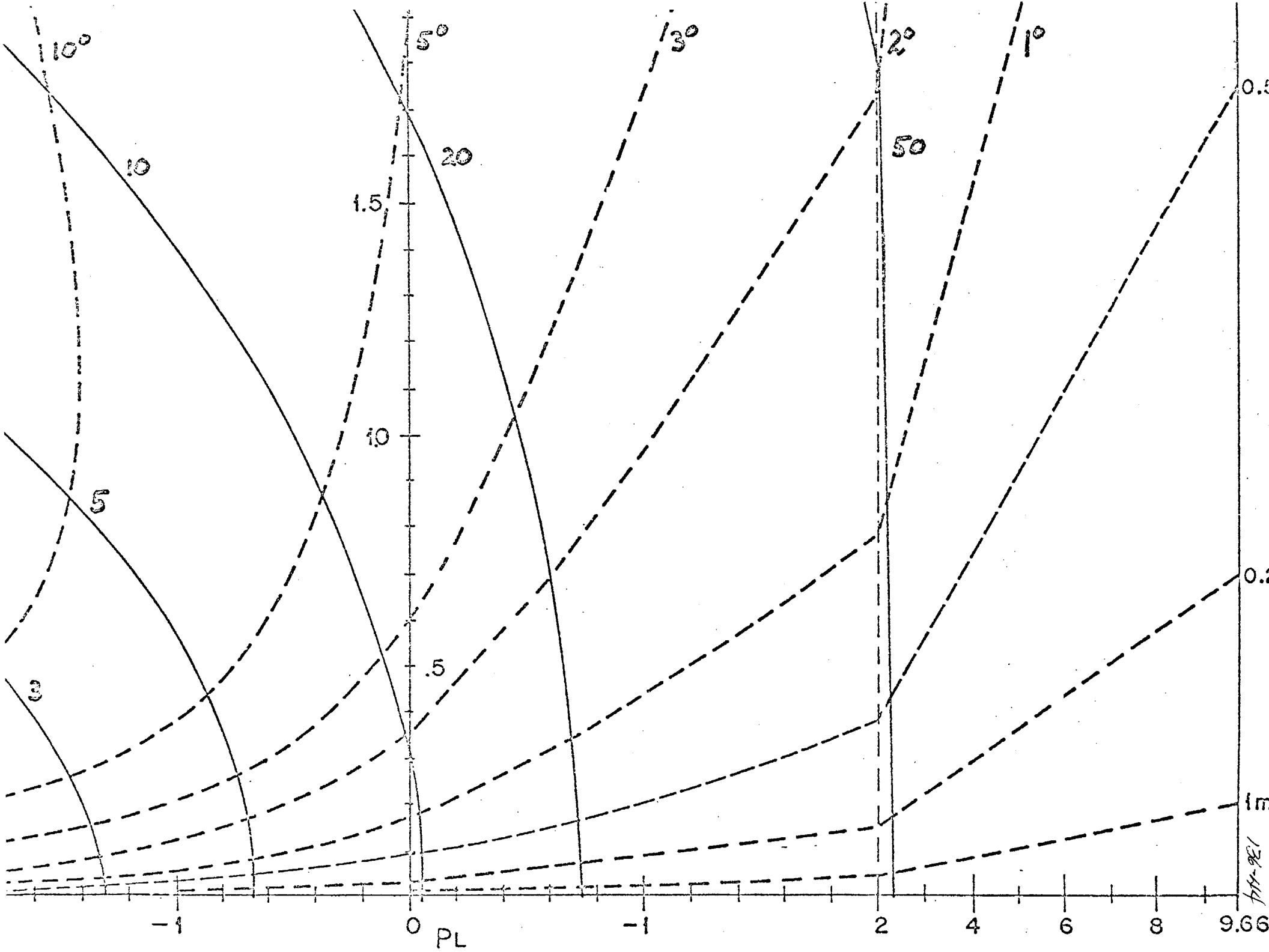

FIG. 4

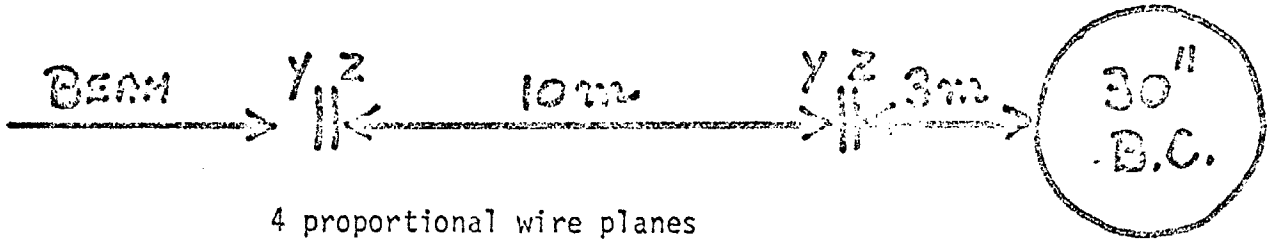

4 proportional wire planes

1 mm wire spacing

2"x2", 50 wires. This can be scaled up by a factor 2 in y if needed.

The momentum defining proportional chamber is not shown, being over 1000' upstream at a focus where the image of the target is ~2 mm in size. The dispersion is ~2 "/% at this point.

Figure 5

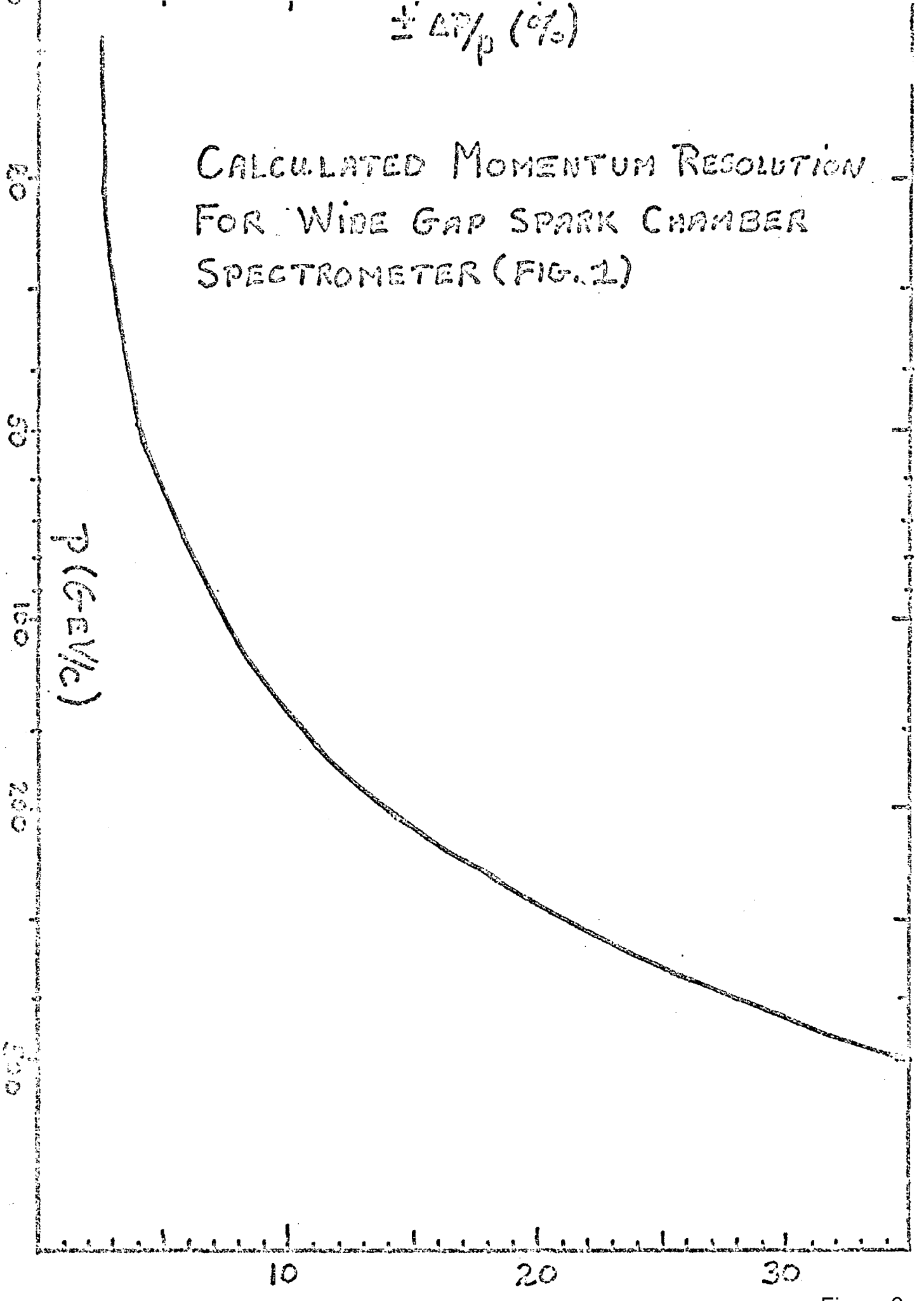
± Δp/p (%)
CALCULATED MOMENTUM RESOLUTION
FOR WIDE GAP SPARK CHAMBER
SPECTROMETER (FIG. 2)
p (GeV/c)
10
20
30

Figure 6

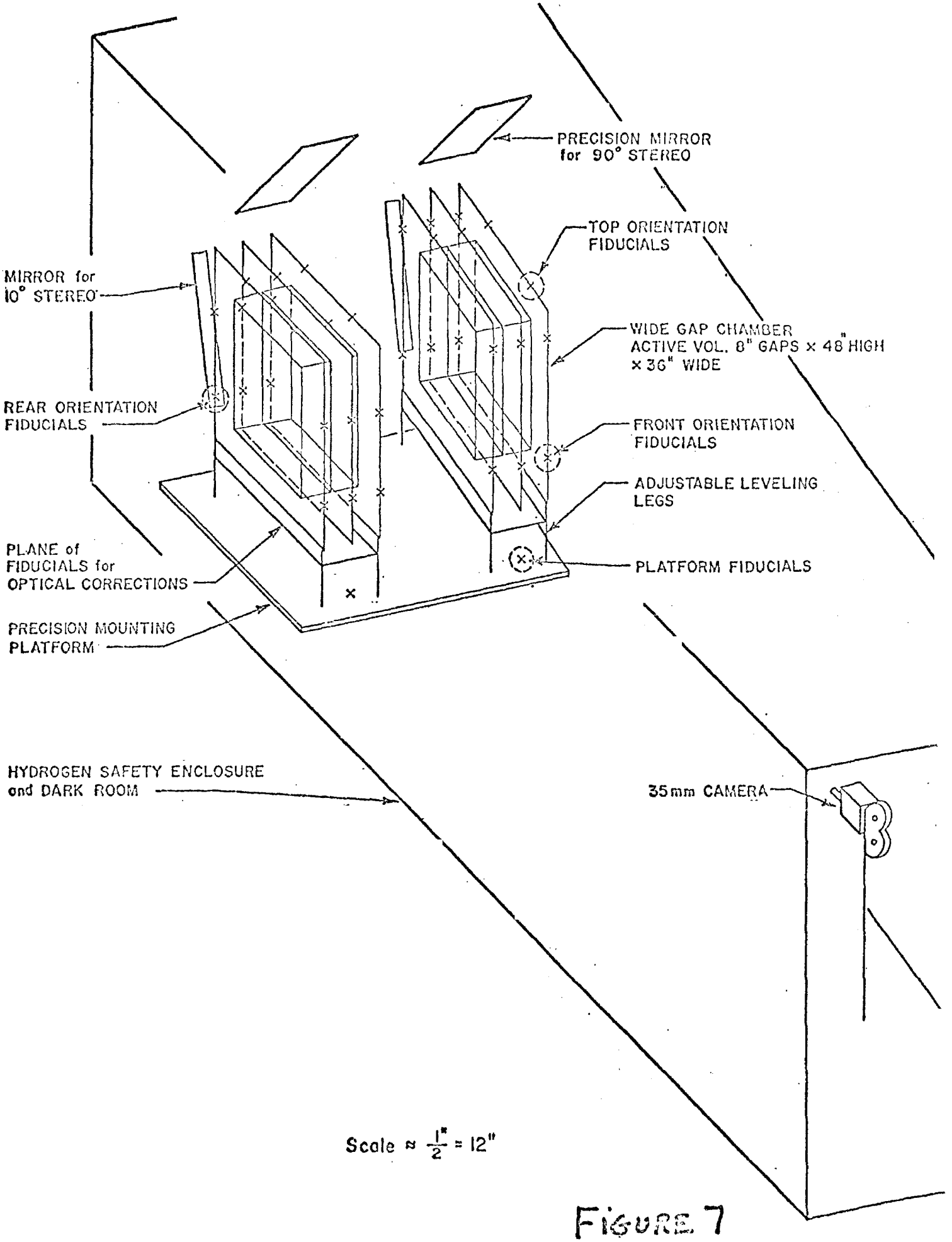

Scale ≈ $\frac{1}{2}$" = 12"

FIGURE 7

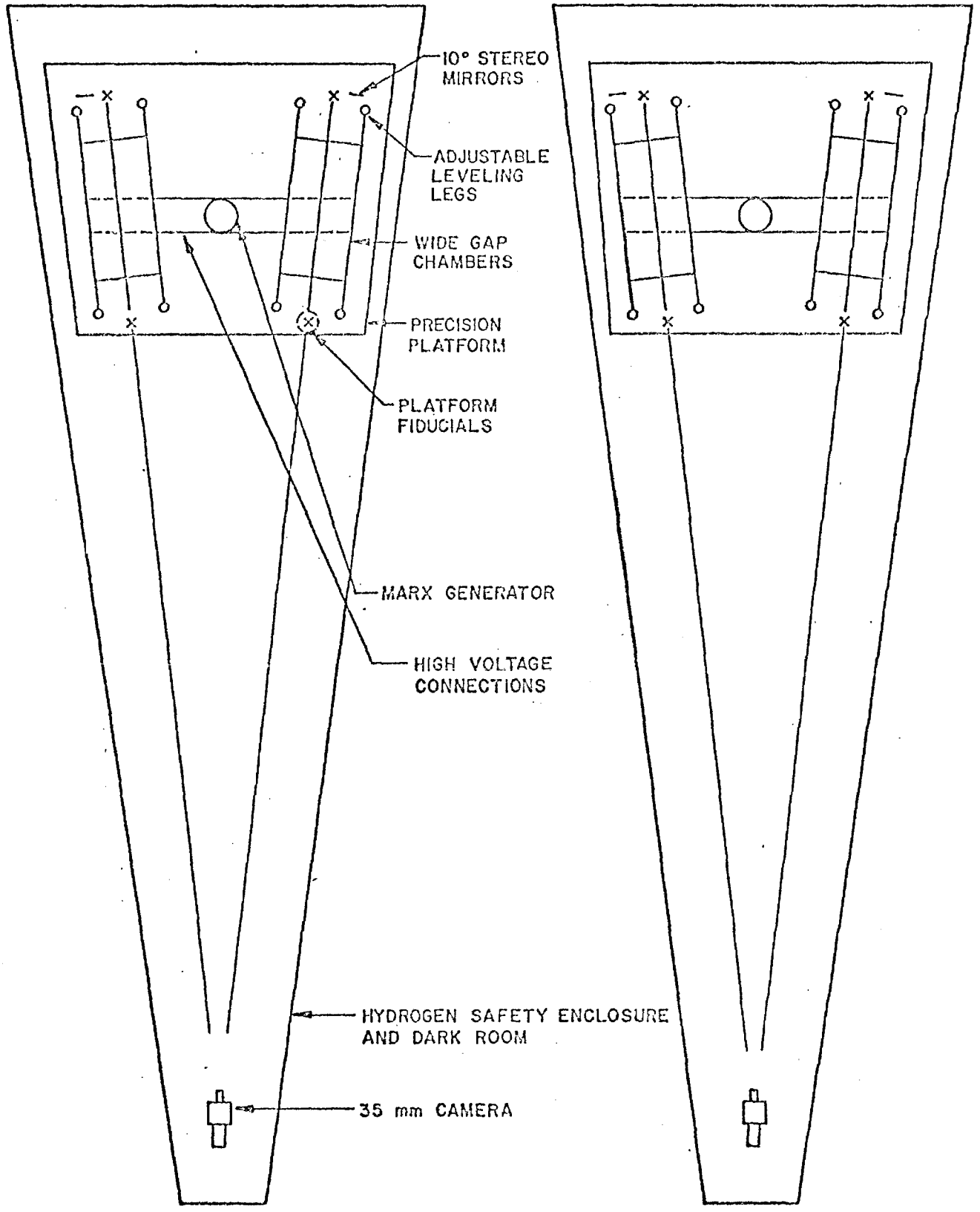

PLAN VIEW
SCALE ≈ $\frac{1}{2}$" = 12"

Figure 8

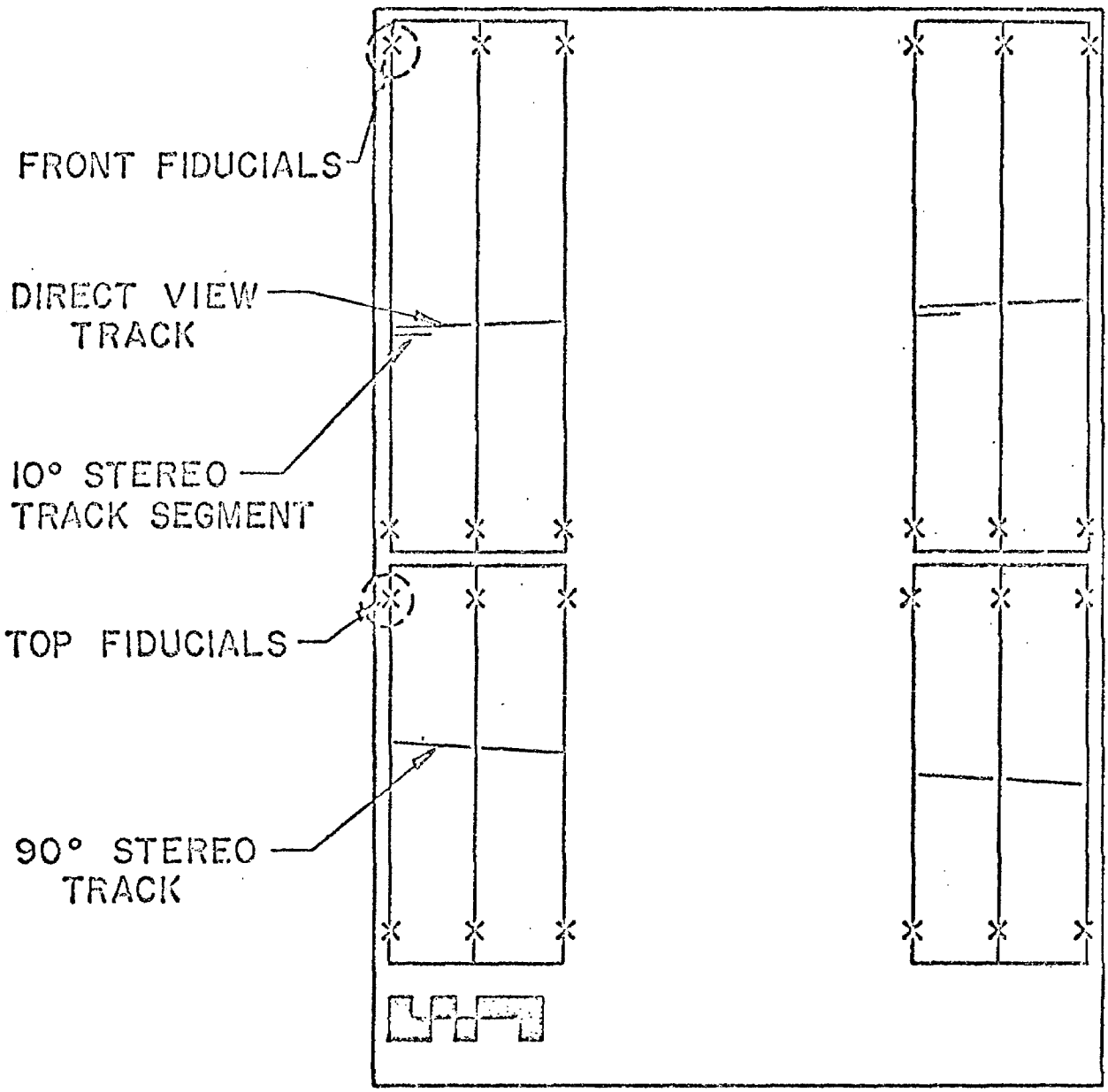

FILM FORMAT 35 mm 1.5" × 1.0"

Figure 9